doi:10.1016/j.jmb.2007.10.068 J. Mol. Biol. (2008) 375, 764–772

JMB

Available online at www.sciencedirect.com

ScienceDirect

ELSEVIER

Predicting the Magnitude of the Reflex Response to Insertions in Ubiquitin

Debra M. Ferraro and Andrew D. Robertson*

Department of Biochemistry, Roy J. and Lucille A. Carver College of Medicine, University of Iowa, Iowa City, IA 52242, USA

Received 20 June 2007; received in revised form 25 October 2007; accepted 26 October 2007
Available online
1 November 2007

Edited by C. R. Matthews

The ability to predict the structural response of a protein to an insertion would be a significant advance for the fields of homology modeling and protein design. However, the effects of insertions on protein conformation are not well understood. Previous work has demonstrated that for two loops in ubiquitin, the primary determinant of the structural adaptation to insertions is the insertion site rather than the sequence of the insertion; this phenomenon was termed the reflex response of loops to insertions. We report herein the analysis of ubiquitin mutants with insertions in two other loops. This study demonstrates that the insertion site is the primary determinant of the response to insertions for these two new loops as well, which further supports the reflex response hypothesis. We also attempted to predict the relative magnitudes of the responses at each site but were unsuccessful. Using the additional data collected in this work, we have refined our predictive hypothesis.

Keywords: insertions; homology modeling; NMR; ubiquitin; protein engineering

Introduction

Insertions and deletions, collectively referred to as indels, are common evolutionary changes in proteins and these changes must often be addressed in homology modeling of proteins with unknown structures.[1] Indels can be used to produce changes in protein structure that are not accessible by point mutation alone,[2] and to add a new function to a protein,[3–5] making indels useful in protein engineering. However, many challenges remain in predicting the effects of insertions and deletions on the remainder of the protein structure.[6] Small insertions (one to four amino acids) have been studied systematically,[7] but more work is needed with larger insertions. To address these challenges, we recently embarked on a systematic experimental investigation of how insertions are accommodated in ubiquitin:[8,9] many of the structurally homologous ubiquitin-like proteins and domains include insertions relative to ubiquitin.

We previously created 10 insertional mutants of ubiquitin.[8] The insertions were placed between residues 9 and 10 and between residues 35 and 36, where insertions occur in other proteins in the ubiquitin fold family. Homologous sequences were taken from these proteins and inserted in the corresponding site in ubiquitin. To explore the influence of the insertion sequences, nonhomologous insertions were made by placing the insertion in the other site or by inserting eight glycines. These mutants were analyzed by NMR chemical shift analysis[8] and X-ray crystal structures were solved for four of the mutants.[9] The results showed that the structural response of ubiquitin to insertions in the 9–10 loop and the 35–36 loop is determined primarily by the insertion site rather than the sequence of the insertion. We have termed this property the reflex response of a protein to insertion in a given site. To test the hypothesis that this reflex response is a general phenomenon, the present study focuses on insertions made between residues 46 and 47 and between residues 61 and 62 of ubiquitin (Fig. 1). We have also used observations

*Corresponding author. E-mail address: andyr@keystonesymposia.org.

Present address: A. D. Robertson, Keystone Symposia, P.O. Box 1630, Silverthorne, CO 80498, USA.

Abbreviations used: HSQC, heteronuclear single quantum coherence; MALDI-TOF, matrix-assisted laser desorption ionization time-of-flight.

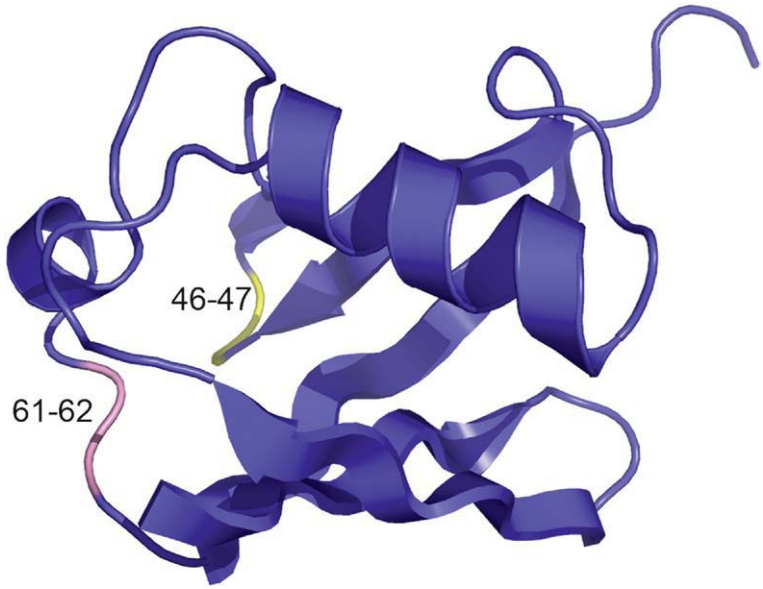

Fig. 1. Locations of the 46–47 and 61–62 loops in ubiquitin. The 46–47 loop is shown in yellow and the 61–62 loop is shown in pink.

from the previous studies of 9–10 and 35–36 loop mutants to try to predict the relative magnitude of the conformational changes in response to insertions at the 46–47 and 61–62 loops.

We selected the 46–47 and 61–62 loops of ubiquitin as insertion sites because insertions occur at these locations in structurally homologous proteins. We placed a homologous insertion from c-Raf1 into the 46–47 loop and a homologous insertion from Elongin B into the 61–62 loop. c-Raf1 is a serine/threonine kinase involved in many signal transduction pathways.[10] Elongin B is an RNA polymerase II transcription factor that has been identified as a target of the von Hippel–Lindau tumor suppressor.[11] In addition, we inserted an octaglycine sequence at each site for direct comparison with our previous studies of octaglycine insertions at the 9–10 and 35–36 sites (Table 1).[8]

Trends from our previous work were used to hypothesize why the structural response to insertions at a given loop is of a large or small magnitude. We first hypothesized that a dynamic loop is able to accept insertions with fewer conformational adjustments throughout the protein than is the case for an inflexible loop. The flexibility of a loop can be examined by hydrogen exchange rates and crystallographic *B*-factors: faster exchange rates indicate a more flexible loop and higher *B*-factors can imply greater flexibility. We also hypothesized that the greater the extent of global interactions of a loop with sequentially distant regions of the protein, the greater the conformational response to insertions at that loop. In this study, we enumerated these interactions by identifying the number of global hydrogen bonds made between the loop and sequentially distant residues and by a simple characterization of the loop conformation: a hairpin loop allows fewer interactions with the remainder of the protein, while an extended loop is capable of forming interactions with the rest of the protein.[12]

We predicted the magnitude of the response to insertions in the 46–47 and 61–62 loops based upon the four factors outlined above: hydrogen exchange rates, *B*-factors, presence of global hydrogen bonds and loop conformation. We considered these factors to be additive, so each loop has zero to four factors indicating a large, global response to insertions at that site. The greater the number of global response factors associated with a loop, the larger and more global the response to insertions at that loop is predicted to be.

The 46–47 loop has two factors associated with it that predict a global conformational response to insertions: low *B*-factors and hydrogen bonds to sequentially distant residues, which we will term global hydrogen bonds. The 61–62 loop has three factors that indicate a large response to insertions: slower hydrogen exchange rates, global hydrogen bonds and an extended loop conformation. In comparison, the 9–10 loop shows little that would indicate a global response, while the 35–36 loop has all four. Therefore, we predicted that the 46–47 loop would have a diminished conformational response to insertions relative to the 61–62 site and that both responses would fall between those observed in the 9–10 and 35–36 loops.

Table 1. Insertion mutants created

Mutant	Insertion site	Inserted sequence[a]	Homologous[b]
46–47 G8	46–47	rlifaGGGGGGGGgkqle	No
46–47 c-Raf1	46–47	rlifaLLHEHKGKgkqle	Yes
61–62 G8	61–62	sdyniGGGGGGGGqkest	No
61–62 Elongin B	61–62	sdyniTSQTARPqkest	Yes

[a] Inserted residues are capitalized and wild-type residues are lowercase.
[b] Insertion sequence derived from structurally homologous position in a ubiquitin-like protein.

Results

Heteronuclear single quantum coherence analysis of structure

We used heteronuclear single quantum coherence (HSQC) spectra to analyze the structural changes made in response to insertions relative to wild-type ubiquitin; changes in HSQC chemical shift are indicative of modest structural changes in proteins.[13] The HSQC spectrum of the 46–47 G8 mutant looks very similar to that for wild-type ubiquitin, with only a few cross-peaks moving significantly (Fig. 2a). At concentrations suitable for NMR experiments, some of the 46–47 c-Raf1 mutant precipitates within a few hours at room temperature. Also, a number of small additional peaks occur in the spectrum. Mass spectrometry of the protein shows additional species that correspond to degradation from the C terminus of the protein, which is the likely cause of the additional peaks. However, the primary peaks show few changes in structure relative to wild type (Figs. 3a and 4a). As we observed previously with the 9–10 loop and the 35–36 loop, the responses apparent in the HSQC spectra are very similar in the two different mutants with insertions in the 46–47 loop. The residues at which a significant change in chemical shift occurred were located near the insertion site (Fig. 3c).

Both the 61–62 G8 mutant and the 61–62 Elongin B mutant also display a set of smaller peaks in addition to the peaks that are similar to those in the wild-type spectrum. Unlike 46–47 c-Raf1, the protein remains soluble, and mass spectrometry indicates that there is only one protein species present in each sample. In order to determine if self-association accounts for the extra peaks, we collected HSQC spectra at a lower concentration of protein (0.2 mM compared to the usual 1 mM) and compared the ratios of peak volumes for each mutant in the two spectra: if self-association is responsible for the two sets of peaks, then decreasing protein concentration should decrease the concentration of multimers and, consequently, change the relative peak volumes for major and minor species. For each mutant, these volume ratios were unchanged at the lower concentration, suggesting that self-association is probably not responsible for the second set of peaks. We propose that the insertion in the 61–62 loop allows an alternate conformation of the protein to become significantly populated.

The structural locations of the residues with extra peaks indicate that the alternate conformation may involve a slight change in the interaction of the helix with the neighboring β-strands as well as some repacking of the hydrophobic core (Fig. 5). The ability of 61–62 loop insertion mutants to access a second conformation may be due to the position of residue 61 in the protein: this isoleucine side chain is buried in the hydrophobic core of ubiquitin, and if the insertion causes the isoleucine to shift from the core, then this may reduce conformational constraints on the remainder of the core, thereby permitting a nearly isoenergetic alternative conformation. We observed a qualitatively similar conformational readjustment in the X-ray structures of ubiquitin variants with insertions between residues 35 and 36.[9]

The response of the 61–62 G8 mutant to the insertion was minimal as well (Fig. 2b). Because multiple conformations are observed, several residues had two opportunities to show a significant change in chemical shift from wild type, as both the peak corresponding to the major conformation and the peak corresponding to the minor conformation could display a significant shift from wild-type values. Of these, only one residue (residue 61) showed a significant change in chemical shift in the peak corresponding to the minor conformation

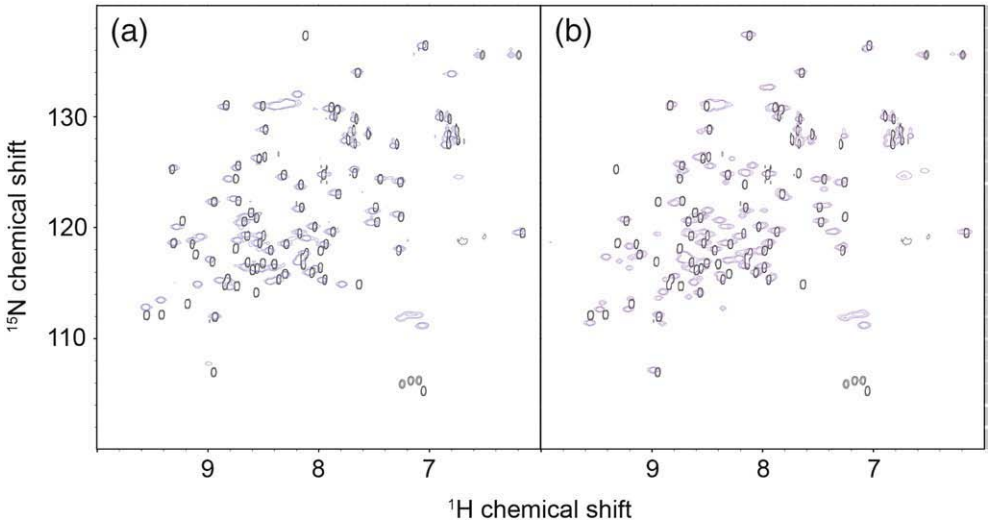

Fig. 2. Wild-type ubiquitin HSQC *versus* insertion mutant HSQC spectra. (a) 46–47 G8 HSQC spectrum (purple) overlaid with wild-type ubiquitin HSQC spectrum (black). (b) 61–62 G8 HSQC spectrum (purple) overlaid with wild-type ubiquitin HSQC spectrum (black).

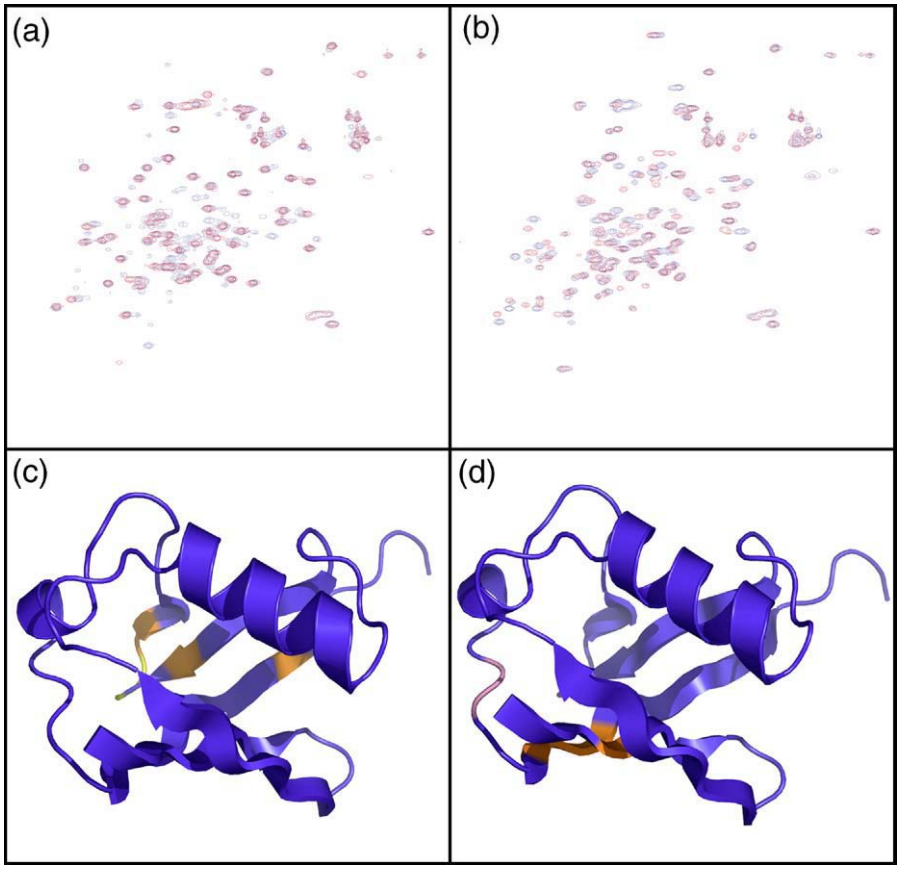

Fig. 3. Insertion-site-specific changes in chemical shift. (a) Overlay of both 46–47 loop insertion mutant HSQC spectra. (b) Overlay of both 61–62 loop insertion mutant HSQC spectra. (c) Locations of residues with significant changes in HSQC chemical shift in response to insertions in the 46–47 loop. A significant change is defined by $[(\Delta^1H)^2 + (0.2 \times \Delta^{15}N)^2]^{1/2} \geq 0.3$ ppm. Residues with changes are shown in orange, and the 46–47 loop is shown in yellow. (d) Locations of residues with significant changes in HSQC chemical shift in response to insertions in the 61–62 loop. Residues with changes are shown in orange and the 61–62 loop is shown in pink.

while showing no significant change in chemical shift relative to wild type in the peak corresponding to the major conformation. In other words, the alternate conformation does not appear to have a significantly different structure from the primary conformation as detected by NMR. 61–62 Elongin B responded in a manner very similar to 61–62 G8 (Figs. 3b and 4b); residues that changed in chemical shift were located near the 61–62 loop (Fig. 3d).

Hydrogen exchange analysis of stability

Protein stability was measured by EX2 hydrogen exchange as described previously.[8] Briefly, the documented correlation between ΔG_{op} (the free energy of the conformational change that opens an amide hydrogen to exchange) and ΔG_u was used to infer the stability of the protein from the measured exchange rates of the slowest exchanging amide hydrogen atoms in the protein.[14] The stability of 46–47 c-Raf1 could not be measured through hydrogen exchange due to its tendency to precipitate at room temperatures (Table 2). The stability of 46–47 G8 was found to be 6.80±0.13 kcal/mol, a decrease of about 2.75 kcal/mol relative to wild-type stability[8] (Fig. 6).

The analysis of the 61–62 loop insertion mutant stabilities is more complicated due to the alternate conformation. The following reasoning allows us to use hydrogen exchange to determine the stability of the most stable conformation when two conformations contribute to exchange of a proton. If k_{obs} is the sum of the individual k_{obs} values for the opening to exchange from each conformation:

$$k_{obs,total} = k_{obs,1} + k_{obs,2} \quad (1)$$

then the fastest motion leading to exchange dominates the observed rate of exchange. Under EX2 exchange conditions, k_{obs} is related to the equilibrium constant for opening, K_{op}, through the equation:

$$k_{obs} = K_{op} k_{rc} \quad (2)$$

where k_{rc} is the intrinsic rate constant for exchange for a given residue, which can be calculated for a given residue based upon the protein sequence.[15] Since the k_{rc} value for a residue will be equivalent for all conformations, we can say:

$$k_{obs,total} = (K_{op,1} + K_{op,2}) k_{rc} \quad (3)$$

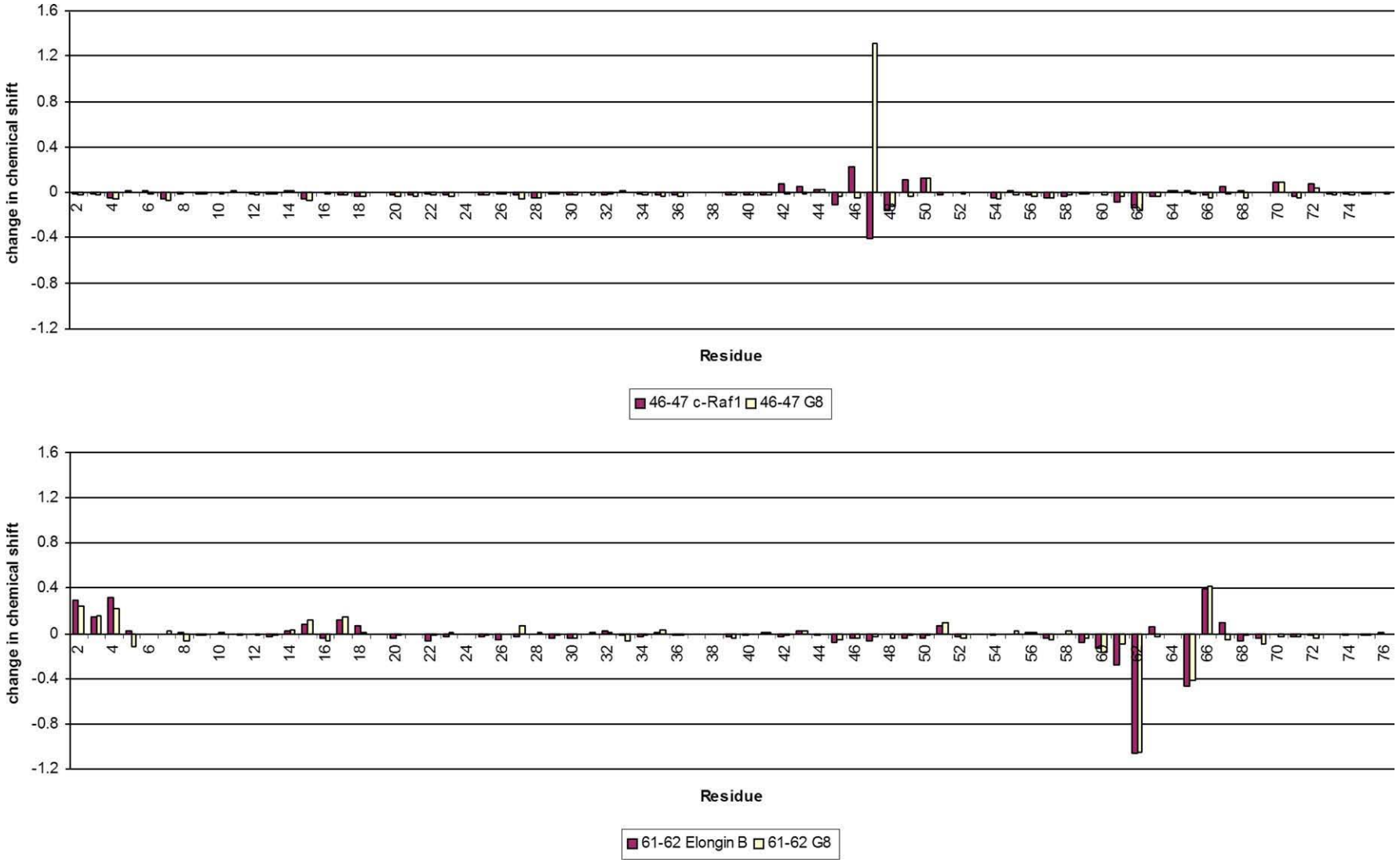

Fig. 4. Change in ^{1}H chemical shift in the 46–47 and 61–62 loop mutants by residue. Changes in chemical shift were calculated by subtracting the mutant chemical shift from the wild-type ubiquitin chemical shift.

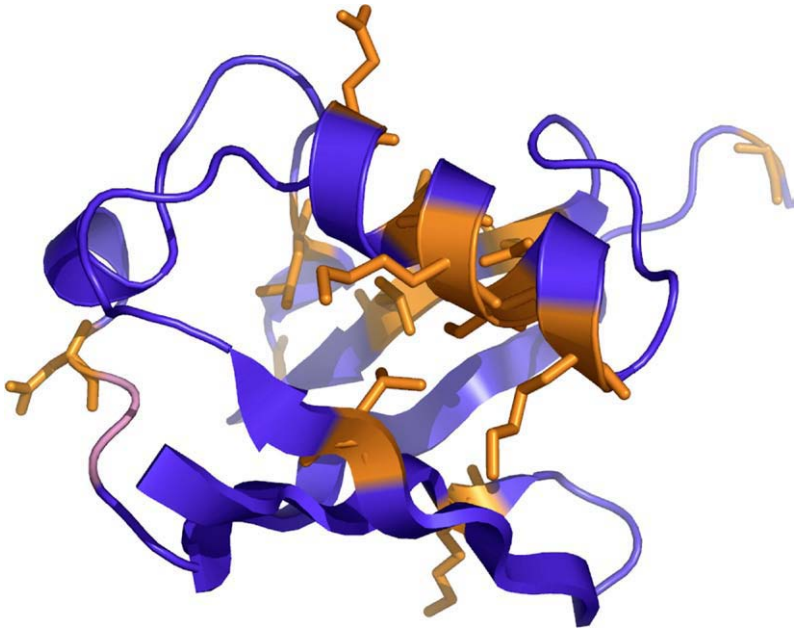

Fig. 5. Residues with an additional HSQC peak in response to insertions in both of the 61–62 loop mutants. The residues that display a second peak are shown in orange with side chains displayed. The 61–62 loop is shown in pink.

The ratio of peak volumes for the major and minor species for each 61–62 loop mutant studied is approximately 2:1. K_{op} for the slowest exchanging amide hydrogen atoms in a protein has been demonstrated to be equivalent to K_u for the protein,[14] thus:

$$K_{op} = K_u = \frac{[U]}{[N]} \quad (4)$$

The unfolded state is the same for both conformations, and the native population of the more stable conformation, $[N_1]$, is twice as large as $[N_2]$, so $2K_{u,1} = K_{u,2}$. Substituting into Eq. (3), we get:

$$k_{obs,total} = (3K_{u,1})k_{rc} \quad (5)$$

which yields the stability of the most stable conformation of the protein. The stabilities determined for the two mutants are 7.16±0.54 kcal/mol for 61–62 G8 and 6.62±0.24 kcal/mol for 61–62 Elongin B (Fig. 6).

Discussion

HSQC analysis of structure

The HSQC spectra of both 61–62 loop mutants changed relative to wild type in a similar manner. In fact, both mutants appeared to have an alternate conformation significantly populated. The reflex response previously observed in the 9–10 and 35–36 loops of ubiquitin therefore appears to apply to the 61–62 loop as well.

The two 46–47 loop insertion mutants showed different characteristics. 46–47 G8 was very similar to wild-type ubiquitin. However, 46–47 c-Raf1 precipitated out of solution at high concentrations (>1 mg/ml) and high temperatures (>20 °C). This precipitation could be due to the highly basic character of the insertion sequence. In c-Raf1, the β-strand nearest the insertion has many hydrogen bond acceptors and negative charges available for interaction with the positive charges in this insertion sequence. In ubiquitin, however, these residues are more hydrophobic and are unlikely to stabilize the

Table 2. Stabilities of insertion mutants

	ΔG_{op} (error) (kcal/mol)	$\Delta\Delta G_{op}$ (kcal/mol)
Wild type	9.3 (0.1)	–
46–47 G8	6.8 (0.1)	−2.5
46–47 c-Raf1	Not determined	Not determined
61–62 G8	7.2 (0.5)	−1.8
61–62 Elongin B	6.6 (0.2)	−2.7

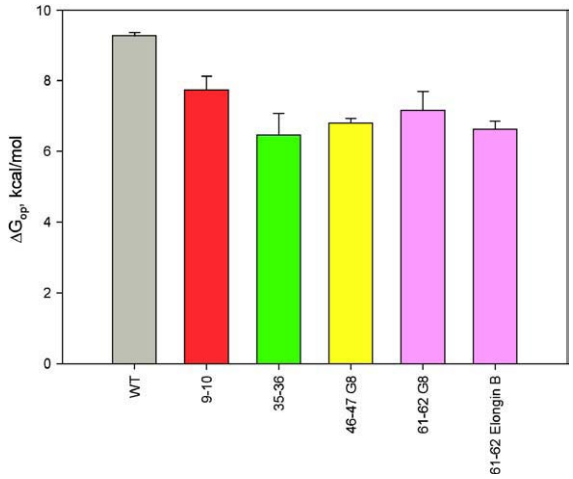

Fig. 6. Stability of insertion mutants relative to wild-type ubiquitin as determined by hydrogen exchange at 45 °C. Error bars represent the standard deviation of the stabilities determined at three different pH values. The values for the 9–10 and 35–36 loops are the averages of all mutants from previously published data.[8]

inserted residues as well. Furthermore, the protein was susceptible to degradation. Nevertheless, the primary peaks in the spectrum, which correspond to folded and soluble protein, had chemical shifts similar to those for 46–47 G8. Therefore, the two 46–47 insertion mutants have similar structures when folded and soluble. In this regard, the reflex response to insertions applies to the 46–47 loop.

Hydrogen exchange analysis of stability

Previously, we hypothesized that the magnitude of the change in stability with insertions at a given loop was correlated to the extent of structural alterations in response to the insertions.[8] For example, this hypothesis would predict that an insertion at a site with more structural perturbations would result in a greater loss of stability. However, the mutants at the 46–47 loop showed fewer structural perturbations than the 9–10 loop mutants, but 46–47 G8 was less stable than the 9–10 loop mutants. Similarly, the 61–62 loop mutants were less perturbed structurally than the 9–10 loop mutants, but they were slightly more destabilized. These results imply that there is no direct correlation between the structural response as observed by NMR and the change in stability brought about by insertions. Perhaps the stability change depends on how well the conformation is able to adapt to the presence of the insertion, regardless of how many residues are altered in the adaptation. The 9–10 loop has the smallest decrease in stability upon insertion in that loop. This may be explained by its location near a terminus of the protein and the room available near the loop to adjust its position, which could allow it to make necessary adjustments in response to insertions effectively without interfering with the rest of the protein.

Accuracy of predictions

We predicted that the 9–10 loop would have the smallest structural response to insertions, followed by the 46–47 loop, the 61–62 loop, and the 35–36 loop. To test the prediction, we found the average number of residues that have a significant change in chemical shift upon insertion per mutant for a given loop, with a significant change defined as $[(\Delta^1H)^2 + (0.2 \times \Delta^{15}N)^2]^{1/2} \geq 0.3$ ppm.[16] Because of the alternate conformations observed in the 61–62 loop mutants, we observed two peaks for certain residues. To account for both sets of peaks, a second data set was created for each of the 61–62 loop mutants, substituting the second set of peaks for each applicable residue.

The number of residues that change chemical shift upon insertion at each loop is shown in Table 3. Both the 46–47 loop and the 61–62 loop mutants had fewer residues with significant changes in response to insertion than either the 9–10 loop or the 35–36 loop mutants. This is not as we predicted. Although the relative magnitudes of the response to insertions in the 46–47 and 61–62 loops were predicted correctly, the predicted relationship to the 9–10 and 35–36 loops was not accurate.

Table 3. Average number of residues that show a significant change in chemical shift upon insertion at a given loop and their average distance from the insertion site

Loop	No. of mutants	Changed residues	Range	Distance (Å)
9–10	5	6.6	6–7	7.6
35–36	5	13.6	9–16	11.1
46–47	2	4.0	3–5	10.2
61–62	4	4.25	3–5	7.6

Interestingly, the average distance of the perturbed residues from the insertion point (measured from the carbonyl carbon of the peptide bond where the insertions were made to the alpha carbon of the affected residue) is greater for the 46–47 loop than for the 61–62 loop, even though essentially the same number of residues were perturbed for each loop; the perturbed residues in the 46–47 loop were at a greater distance from the loop than those in the 61–62 loop mutant (Fig. 3c). This distinction has interesting implications in allostery; perturbations at certain sites appear to be more likely to cause allosteric changes at a distance, regardless of the number of residues affected.

With the results from the additional two loops studied, we have refined our criteria for predicting the magnitude of structural response to insertions at a given loop. The most intriguing observation is that insertions in the 35–36 loop lead to larger structural perturbations than insertions in any of the other three loops tested. A likely reason for the exaggerated response to insertions at the 35–36 loop is the presence of prolines at residues 37 and 38. Forcing a change in the structure of these highly constrained residues could be quite destabilizing and thus require compensation through a series of global structural changes. None of the other sites are near a proline, indicating that this factor may play a role in the disparity of responses to insertions between the 35–36 loop and the other loops.

It seems reasonable to group the insertion sites into two groups: the exaggerated responders and the subtle responders. The 35–36 loop, having a much larger number of residues that respond to insertions than the other three loops, is the sole exaggerated responder. None of the factors used in the predictions made for this study correlate well with the relative magnitudes of response of the three subtle responders. However, there is essentially no difference between the numbers of residues changed upon insertion at the 46–47 and 61–62 loops, and the numbers of residues that change upon insertion are very close to that of the 9–10 loop. Therefore, given the small number of mutants tested in the 46–47 and 61–62 loops, the differences between the subtle responders may not be significant. In general, results from our studies suggest that a conformationally restricted stretch near the insertion site leads to a larger structural response to insertions.

The apparent allosteric effect observed in the 35–36 loops and the 46–47 loop, where changes are seen at a greater distance from the insertion site, does correlate to a simple structural feature of the loop. In each of these four cases, an insertion in a loop with low crystallographic *B*-factors in relation to the average *B*-factor of a structure produces a distant response, while an insertion at a loop with high crystallographic *B*-factors produces a local response. This makes intuitive sense because a higher *B*-factor indicates more structural disorder in the region, which is likely in this case to correlate to a greater mobility of the region. More flexibility in the loop may allow structural adjustments required to accommodate the insertion to occur within the loop region. This result allows us to hypothesize that insertions in loops with a low *B*-factor (the *B*-factors in the loop averaging about 5–10% lower than the average of the entire protein) cause structural perturbations at a greater distance from the insertion site (>10 Å), while the effects of insertions in loops with a high *B*-factor (again, 5–10% higher than the entire protein) occur within 10 Å from the insertion site.

In this study, we have demonstrated the applicability of the reflex response to other loops in ubiquitin. While our attempts at predicting the relative magnitude of the structural effects of the insertions at each loop were unsuccessful, we were able to use the results to form new hypotheses for further predictions. More important, we upheld our previous hypothesis that the primary determinant for the structural response to an insertion is the sequence of the protein near the loop in which the insertion is made.

Methods

Mutagenesis, expression and purification of mutants

Mutants were created *via* PCR, expressed and purified as described previously.[8] To accommodate the increased T_m of the primers once the insertion was incorporated into the template, the annealing temperature was 5 °C higher for the final 13 cycles of PCR than it was for the first 5 cycles. Unlike the other mutants, 46–47 c-Raf1 required elution from the CM52 column with 100 mM ammonium acetate, pH 7.0. Mutants exhibiting multiple sets of peaks on HSQC spectra were analyzed with matrix-assisted laser desorption ionization time-of-flight (MALDI-TOF) mass spectrometry to check for degradation or multiple populations. Samples for mass spectrometry were composed of 0.5 mg/mL protein in a 1:1 water/acetonitrile solution. A Bruker Biflex III MALDI-TOF mass spectrometer at the University of Iowa Molecular Analysis Facility was used.

HSQC analysis

HSQC spectra were collected at 25 °C and analyzed as described previously.[8] The alpha proton chemical shift information gained from HNHA data was used to aid in peak assignments in the HSQC.[17]

Hydrogen exchange studies

Hydrogen exchange was performed as described previously.[8] Briefly, 1 mM protein was transferred to ^2H_2O and brought to a basic pH to initiate exchange, which was monitored by 1-D NMR spectra. The rate of decay of the peaks was used to determine ΔG_{op} for each slowly exchanging amide hydrogen. The ΔG_{op} values from the three most stable amide hydrogen atoms for each mutant under each pH condition were averaged to yield ΔG_u for the protein at that condition [14]. The amide hydrogen atoms yielding the most stable ΔG_{op} values were always among the same 10 residues. The values of ΔG_u for each protein at three different pH conditions were averaged to yield the overall ΔG_u for the protein.

Acknowledgement

The study was supported by NIH grant GM46869. D.M.F. is a predoctoral fellow of the Howard Hughes Medical Institute.

References

1. Tramontano, A. & Morea, V. (2003). Assessment of homology-based predictions in CASP5. *Proteins*, **53**, 352–368.
2. Shortle, D. & Sondek, J. (1995). The emerging role of insertions and deletions in protein engineering. *Curr. Opin. Biotechnol.* **6**, 387–393.
3. Kim, Y., Welch, J. T., Lindstrom, K. M. & Franklin, S. J. (2001). Chimeric HTH motifs based on EF-hands. *J. Biol. Inorg. Chem.* **6**, 173–181.
4. Kovacic, R. T., Welch, J. T. & Franklin, S. J. (2003). Sequence-selective DNA cleavage by a chimeric metallopeptide. *J. Am. Chem. Soc.* **125**, 6656–6662.
5. Shields, S. B. & Franklin, S. J. (2004). De novo design of a copper(II)-binding helix–turn–telix chimera: the prion octarepeat motif in a new context. *Biochemistry*, **43**, 16086–16091.
6. Heuser, P., Wohlfahrt, G. & Schomburg, D. (2004). Efficient methods for filtering and ranking fragments for the prediction of structurally variable regions in proteins. *Proteins: Struct., Funct., Bioinf.* **54**, 583–595.
7. Vetter, I. R., Baase, W. A., Heinz, D. W., Xiong, J. P., Snow, S. & Matthews, B. W. (1996). Protein structural plasticity exemplified by insertion and deletion mutants in T4 lysozyme. *Protein Sci.* **5**, 2399–2415.
8. Ferraro, D. M., Hope, E. K. & Robertson, A. D. (2005). Site-specific reflex response of ubiquitin to loop insertions. *J. Mol. Biol.* **352**, 575–584.
9. Ferraro, D. M., Ferraro, D. J., Ramaswamy, S. & Robertson, A. D. (2006). Structures of ubiquitin insertion mutants support site-specific reflex response to insertions hypothesis. *J. Mol. Biol.* **359**, 390–402.
10. Morrison, D. K. & Cutler, J. R. E. (1997). The complexity of Raf-1 regulation. *Curr. Opin. Cell. Biol.* **9**, 174.
11. Aso, T., Conaway, J. W. & Conaway, R. C. (1995). The RNA polymerase II elongation complex. *FASEB J.* **9**, 1419–1428.
12. Tramontano, A., Chothia, C. & Lesk, A. M. (1989). Structural determinants of the conformations of medium-sized loops in proteins. *Proteins*, **6**, 294–382.

13. Wagner, G., Pardi, A. & Wuthrich, K. (1983). Hydrogen bond length and ^{1}H NMR chemical shifts in proteins. *J. Am. Chem. Soc.* **105**, 5948–5949.
14. Huyghues-Despointes, B. M. P., Scholtz, J. M. & Pace, C. N. (1999). Protein conformational stabilities can be determined from hydrogen exchange rates. *Nat. Struct. Biol.* **6**, 910–912.
15. Bai, Y., Milne, J. S., Mayne, L. & Englander, S. W. (1993). Primary structure effects on peptide group hydrogen exchange. *Proteins*, **17**, 75–86.
16. Foster, M. P., Wuttke, D. S., Clemens, K. R., Jahnke, W., Radhakrishnan, I., Tennant, L. *et al.* (1998). Chemical shift as a probe of molecular interfaces: NMR studies of DNA binding by the three amino-terminal zinc finger domains from transcription factor IIIA. *J. Biomol. NMR*, **12**, 51–71.
17. Vuister, G. W. & Bax, A. (1993). Quantitative J correlation: a new approach for measuring homonuclear three-bond J(HNH.alpha.) coupling constants in 15N-enriched proteins. *J. Am. Chem. Soc.* **115**, 7772–7777.